

## Electronic Supplementary Information

### $\alpha$ -MnO<sub>2</sub>/MWCNTs as an electrocatalyst for rechargeable relatively closed system Li-O<sub>2</sub> batteries

Min Wu<sup>abc</sup>, Dechong Liu<sup>a</sup>, Zhuxin Li<sup>a</sup>, Yu Tang<sup>a</sup>, Yajun Ding<sup>bc</sup>, Yuejiao Li<sup>bcd</sup>,  
Zhong-Shuai Wu<sup>\*bc</sup> and Hong Zhao<sup>\*a</sup>

<sup>a</sup>*New Energy Laboratory, Dalian Jiaotong University, 794 Huanghe Road, Dalian  
116028, China*

<sup>b</sup>*State Key Laboratory of Catalysis, Dalian Institute of Chemical Physics, Chinese  
Academy of Sciences, 457 Zhongshan Road, Dalian 116023, China*

<sup>c</sup>*Dalian National Laboratory for Clean Energy, Chinese Academy of Sciences, 457*

<sup>d</sup>*University of Chinese Academy of Sciences, 19 A Yuquan Road, Shijingshan  
District, Beijing, 100049, China*

*Zhongshan Road, Dalian 116023, China*

\*Corresponding author.

E-mail address: zhaohong@djtu.edu.cn (Hong Zhao)

E-mail address: wuzs@dicp.ac.cn (Zhong-Shuai Wu)

#### Materials

Mineral chameleon (KMnO<sub>4</sub>, AR), hydrochloric acid (HCl, AR), tetraethylene glycol dimethyl ether (TEGDME, AR), bis trifluoromethane sulfonyl amine lithium (LiTFSI, AR), polyvinylidene fluoride (PVDF, AR) were all purchased from Aladdin Reagent (Shanghai) Co., Ltd. N-methylpyrrolidone (NMP, AR) was purchased from Acrose. MWCNTs (AR) was obtained from Beijing DeKe Daojin Science and

Technology Co., Ltd.

### **Preparation of $\alpha$ -MnO<sub>2</sub>/MWCNTs**

200 mg KMnO<sub>4</sub> was added into 50 ml of deionized water and heated at 80 °C, then 100 mg MWCNTs were uniformly dispersed into the solution and kept at 80 °C for 24 hours. The pH of the solution was adjusted to 2.5 with 2 mol L<sup>-1</sup> HCl. After washing with deionized water and drying in a vacuum oven at 100 °C for 12 hours, the  $\alpha$ -MnO<sub>2</sub>/MWCNTs catalyst was obtained. The  $\alpha$ -MnO<sub>2</sub>/MWCNTs (1:4) and  $\alpha$ -MnO<sub>2</sub>/MWCNTs (1:8) are the mass ratios of  $\alpha$ -MnO<sub>2</sub>/MWCNTs of 1:4 and 1:8, respectively, while other steps are kept same as  $\alpha$ -MnO<sub>2</sub>/MWCNTs.

### **Material characterization**

X-ray diffraction (XRD) patterns were performed on a PANalytical X'pert Pro with Cu K  $\alpha$  radiation. The surface morphology of the samples was observed by JSM-7800F and TM3030 plus scanning electron microscope (SEM). High resolution transmission electron microscopy (TEM) images and energy-dispersive spectroscopy (EDS) were recorded on JEM-2100F TEM instrument operated. A synchronous thermal analyzer (Mettler TGA/DCS 3) was used to analyze and test the thermal properties of the material. Auto-sorb iQ2 (Quanta Chrome) microporous physical adsorption apparatus was used to analyze the specific surface area and pore structure of catalysts. A Renishaw in Via fiber Raman spectrometer was used to analyze the structure and composition of the samples.

### **Preparation and electrochemical measurement of Li-O<sub>2</sub> batteries**

The Li-O<sub>2</sub> battery was assembled by sandwiching a glass fiber separator (Whatman) between  $\alpha$ -MnO<sub>2</sub>/MWCNTs-based cathode and Li anode soaked with 1 M LiTFSI-

TEGDME electrolyte. The cathode was prepared by coating homogeneous slurry composed of a mixture of 90 wt% as-fabricated  $\alpha$ -MnO<sub>2</sub>/MWCNTs catalysts, 10 wt% of polyvinylidene fluoride (PVDF) on carbon paper, then dried in vacuum oven at 100 °C for 12 hours. The electrochemical performance was evaluated using the CR2032 button-type porous Li-O<sub>2</sub> batteries, which was assembled in a glove box under the protection of an argon atmosphere. Afterwards, the battery was moved into a closed box with a volume of about 8 L, which aerated pure oxygen for 40 minutes, and then aerated high-purity argon for 40 minutes to replace oxygen from the system. The battery was measured after the entire system reaches a relatively closed state. The traditional Li-O<sub>2</sub> batteries transfers the assembled battery to a sealed test container filled with high-purity O<sub>2</sub> for testing. All the capacity and current density values were normalized with the total mass of catalyst and PVDF.

### **In-situ Raman instrumental characterizations**

In-situ Raman was carried out with an air-tight three-compartment spectroelectrochemical cell. The cathode was prepared by coating the slurry of catalyst and polyvinylidene fluoride (PVDF) (with the mass ratio of 9:1) on stainless steel mesh. Then, the cathode was placed behind quartz window. Raman spectra were recorded with a customized LabRAM HR800 confocal Raman microscope (Horiba Jobin Yvon). The spectrometer was equipped with an 18 mW He:Ne 633 nm laser source for excitation, a 1800 or 600 lines/mm grating to disperse the scattering light with different resolutions, and a long working distance objective lens (Nikon 50 x 0.45 NA) to focus laser beam on and collect the scattering light from the electrode

surface.

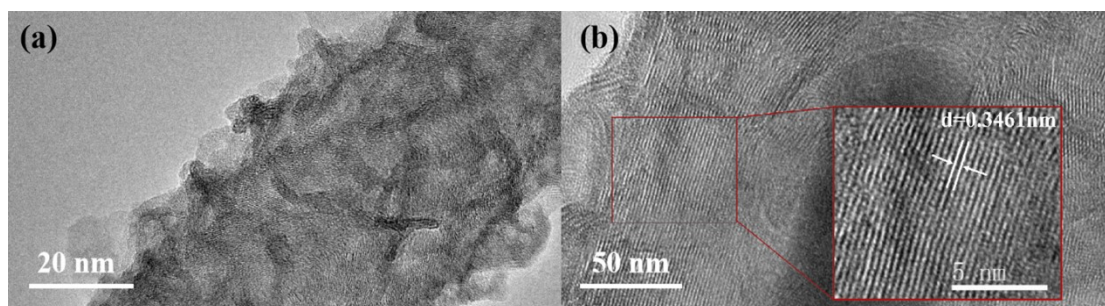


**Fig. S1** (a) TEM image and (b) HRTEM image of the  $\alpha$ -MnO<sub>2</sub>/MWCNTs. Inset in (b) is the corresponding high-magnification HRTEM image.

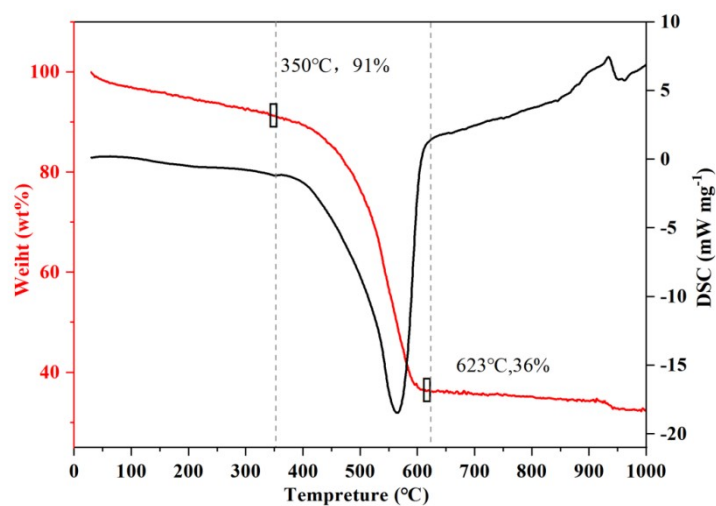


**Fig. S2** TGA and DTG curves of  $\alpha$ -MnO<sub>2</sub>/MWCNTs.

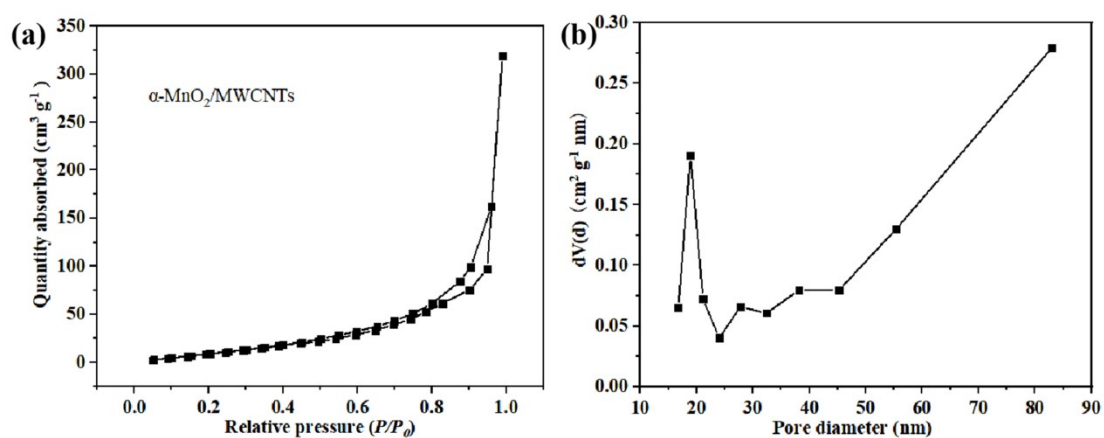


**Fig. S3** (a) Nitrogen adsorption and desorption isotherm and (b) pore size

distribution of  $\alpha$ -MnO<sub>2</sub>/MWCNTs.

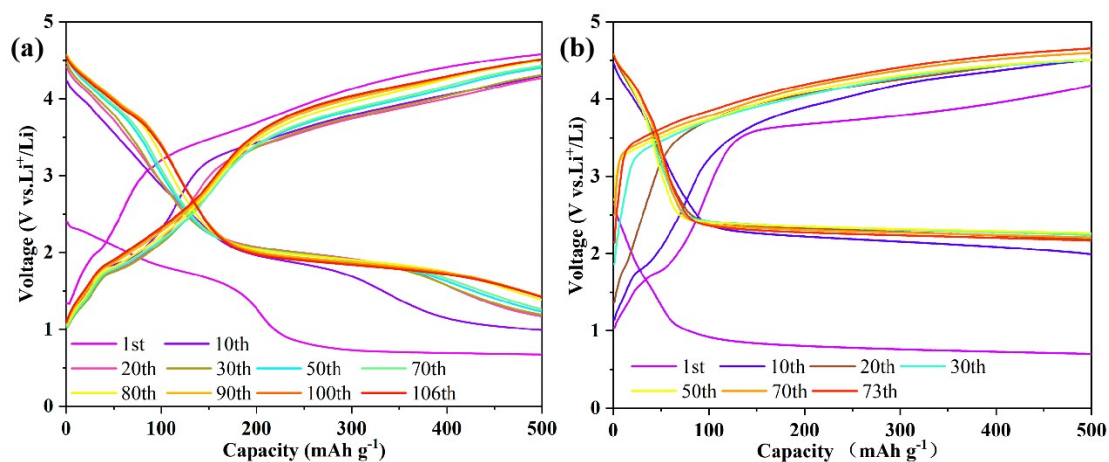


**Fig. S4** Discharge and charge curves of RCLO batteries with a cut-off capacity of 500 mA h g<sup>-1</sup> at 1 A g<sup>-1</sup> of (a)  $\alpha$ -MnO<sub>2</sub>/MWCNTs (1:4) and (b)  $\alpha$ -MnO<sub>2</sub>/MWCNTs (1:8)

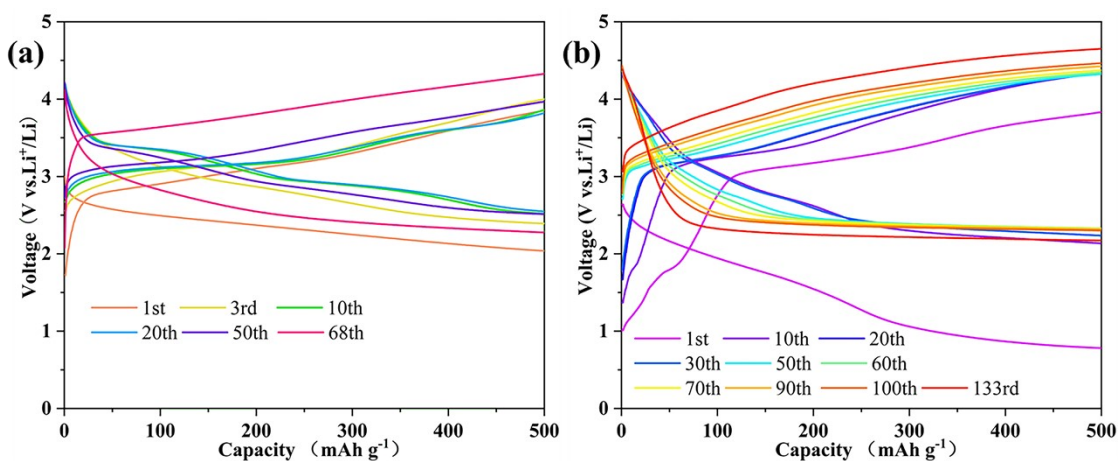


**Fig. S5** Discharge and charge curves with a cut-off capacity of 500 mA h g<sup>-1</sup> at 1 A g<sup>-1</sup> of (a) traditional Li-O<sub>2</sub> batteries and (b) of RCLO batteries

In order to explore the internal electrochemical reaction of RCLO battery, we carried out in-situ Raman spectra characterizations to analyze the evolution of electrochemical products at the  $\alpha$ -MnO<sub>2</sub>/MWCNTs cathode during the discharge and charge processes. At the beginning of the discharge process, the Raman spectra have a characteristic peak of Li<sub>2</sub>O<sub>2</sub> at a frequency of 740 cm<sup>-1</sup> (Fig. S6a).<sup>[1]</sup> When the voltage

reaches the range of 2.4 V to 2.0 V, the characteristic peak of  $\text{LiO}_2$  appears at the frequency of  $1134\text{ cm}^{-1}$ , however, it disappears when the voltage drops below 1.6 V. This phenomenon can be explained from the following three stages. At the first stage, the  $\text{LiO}_2$  was formed from a certain amount of  $\text{O}_2$  adsorbed on the carbon paper when the voltage is 2.4 V. Due to the low  $\text{LiO}_2$  content,  $\text{LiO}_2$  is a weaker peak at 2.4 V. At the second stage, it is observed that with further discharge the  $\text{LiO}_2$  gradually reacts to form  $\text{Li}_2\text{O}_2$  phase. At the third stage, all the  $\text{LiO}_2$  is formed into  $\text{Li}_2\text{O}_2$  when the discharge voltage is lower than 1.6 V. During the charging process (Fig. S6b),  $\text{Li}_2\text{O}_2$  is reversibly formed to  $\text{LiO}_2$ , resulting in a characteristic peak of  $\text{LiO}_2$  in the early charge stage. As the charging progresses, all the  $\text{LiO}_2$  were converted into  $\text{Li}^+$ . After the voltage reaching 3.2 V, the characteristic peak of  $\text{LiO}_2$  disappeared, and the characteristic peak of  $\text{Li}_2\text{O}_2$  gradually weakened after continuous charging. Importantly, this reversible phase interconversion between  $\text{LiO}_2$  and  $\text{Li}_2\text{O}_2$  is stably and periodically appeared after several cycles using the in-situ Raman spectra (Fig. S7). Therefore, it is experimentally evidenced that the interconversion between  $\text{LiO}_2$  and  $\text{Li}_2\text{O}_2$  in a relatively closed system is feasible for practical Li- $\text{O}_2$  battery during the charge and discharge process.

According to the results of Bryan D. McCloskey et al., it is known that PVDF degrades in the presence of reduced oxygen during Li- $\text{O}_2$  discharge. The Raman shift ( $\sim 1133$  and  $1525\text{ cm}^{-1}$ ) formed by this degradation process is almost the same as the reported product of  $\text{LiO}_2$ , which complicates the identification of  $\text{LiO}_2$  in Li- $\text{O}_2$  batteries<sup>[2]</sup>. Therefore, the above analysis of Raman data is only speculation, and its reaction mechanism needs further study.

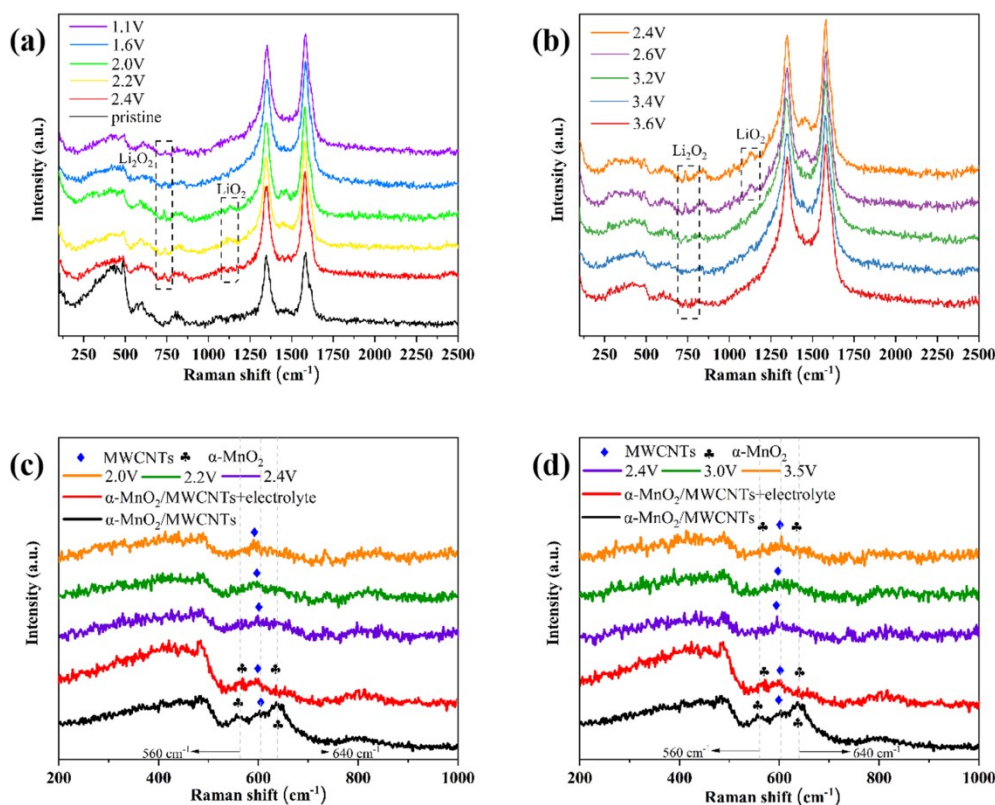


**Fig. S6** (a,b) In-situ Raman spectra of intermediate products in (a) the first discharge process and (b) first charge process. (c,d) In-situ Raman spectra of  $\alpha$ -MnO<sub>2</sub>/MWCNTs catalysts at a current density of 100 mA g<sup>-1</sup> in (c) discharge process and (d) charge process.

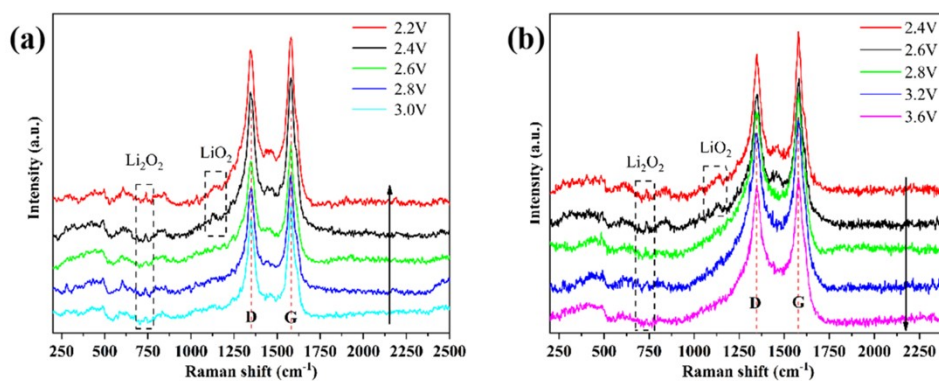


**Fig. S7** In-situ SERS of the  $\alpha$ -MnO<sub>2</sub>/MWCNTs as a cathode catalyst in the RCLO battery after 5th cycles at a current density of 100 mA g<sup>-1</sup> of (a) discharge process and

(b) charge process

## Reference

[1] X.-B. Han, K. Kannari and S. Ye, *Current Opinion in Electrochemistry* **2019**, *17*, 174-183.

[2] J. K. Papp, J. D. Forster, C. M. Burke, H. W. Kim, A. C. Luntz, R. M. Shelby, J. J. Urban and B. D.

McCloskey, *J Phys Chem Lett* **2017**, *8*, 1169-1174.